FEM modelling to predict spatiotemporally resolved water uptake in organic coatings

Experimental validation by odd random phase electrochemical impedance spectroscopy measurements

Meeusen, M.; van Dam, J. P.B.; Madelat, N.; Jalilian, E.; Wouters, B.; Hauffman, T.; Van Assche, G.; Mol, J. M.C.; Hubin, A.; Terryn, H.

DOI
10.1016/j.porgcoat.2023.107710

Publication date
2023

Document Version
Final published version

Published in
Progress in Organic Coatings

Citation (APA)
Meeusen, M., van Dam, J. P. B., Madelat, N., Jalilian, E., Wouters, B., Hauffman, T., Van Assche, G., Mol, J. M. C., Hubin, A., & Terryn, H. (2023). FEM modelling to predict spatiotemporally resolved water uptake in organic coatings: Experimental validation by odd random phase electrochemical impedance spectroscopy measurements. *Progress in Organic Coatings*, *182*, Article 107710. https://doi.org/10.1016/j.porgcoat.2023.107710

Progress in Organic Coatings 182 (2023) 107710

Contents lists available at ScienceDirect

Progress in Organic Coatings

journal homepage: www.elsevier.com/locate/porgcoat

FEM modelling to predict spatiotemporally resolved water uptake in organic coatings: Experimental validation by odd random phase electrochemical impedance spectroscopy measurements

M. Meeusen [a,*], J.P.B. van Dam [b], N. Madelat [a], E. Jalilian [c], B. Wouters [a], T. Hauffman [a], G. Van Assche [c], J.M.C. Mol [b], A. Hubin [a], H. Terryn [a]

[a] Research Group of Electrochemical and Surface Engineering (SURF), Dept. Materials and Chemistry, Vrije Universiteit Brussel, 1050 Brussels, Belgium
[b] Department of Materials Science and Engineering, Delft University of Technology, 2628 CD Delft, the Netherlands
[c] Research Group of Physical Chemistry and Polymer Science (FYSC), Dept. Materials and Chemistry, Vrije Universiteit Brussel, 1050 Brussels, Belgium

ARTICLE INFO

Keywords:
Water transport
Impedance
Coatings
FEM
Comsol Multiphysics

ABSTRACT

In this work, a new finite element modelling (FEM) approach is followed to model spatiotemporally resolved water uptake in organic coatings. To this aim, we start from a physical model, where not only Fickian diffusion of water is taken into account but also the adsorption/desorption reaction of water on the polymer matrix. Starting from a number of important coating properties and crucial model parameters, derived from gravimetric and Fourier transform infrared (FTIR) measurements as the model input, the local water concentration over the coating thickness as a function of time is modelled for a polyethylene glycol diacrylate (PEGDA) coating. The modelled water concentration is then used to calculate virtual capacitance values which are evaluated against experimental capacitance values extracted from impedance measurements. The constraints of the FEM model and ORP-EIS experiments and the discrepancies between them are critically discussed in order to carry out a meaningful model validation, eventually leading to model improvements.

1. Introduction

An important aspect defining durability and lifetime of organic coatings is the description of transport phenomena (of water and ions) through their polymeric networks since these are considered to be a key process in coating failure. One way to describe and predict these phenomena is by predictive modelling. Current predictive models developed for coating assessment are mainly focussed on water uptake over time [1,2]. However, the present state of the art is limited to modelling strictly based on Fickian diffusion and comparing this with experimentally obtained water uptake values obtained from experimental techniques without a critical appraisal of the reliability of the model validation [1,2].

The transport of electrolyte in polymer coatings has been studied experimentally with a range of techniques including gravimetric, Fourier transform infrared (FTIR) spectroscopy and electrochemical impedance spectroscopy (EIS) measurements [1,3–5]. Gravimetry and FTIR spectroscopy are both capable of following the water uptake kinetics, expressed as mass water uptake versus time, and allow the determination of the related diffusion coefficient [6]. EIS adds to this as it allows a powerful quantitative evaluation for the analysis of changes in coating capacitance and associated dielectric properties during water uptake [2,7,8].

Investigation of the water absorption mechanism in polyethylene glycol diacrylate (PEGDA) films proves to follow a typical two-stage sorption process, initially governed by Fickian diffusion, followed by polymer swelling [6,8]. It is widely accepted that water in hydrophilic polymers can be present in two-states: free and bound water [9] and consequently the distinction between them is made when modelling moisture uptake in polymer matrix systems [10–12]. As such the adsorption and desorption reaction of water in the polymer matrix has been described based on an adapted Langmuir isotherm as a function of its adsorption and desorption rate constants and their respective surface coverage [13,14].

In this work, we aim to develop and validate a finite element model (FEM), able to predict the spatiotemporal water distribution within organic coatings based on a number of important coating properties as well as gravimetric and FTIR measurements to estimate the relevant

* Corresponding author.
E-mail address: Mats.Meeusen@vub.be (M. Meeusen).

https://doi.org/10.1016/j.porgcoat.2023.107710
Received 22 March 2023; Received in revised form 12 May 2023; Accepted 26 May 2023
Available online 3 June 2023

model parameters. Solving the mass conservation equation for the water uptake of a (PEGDA) coating allows the prediction of the local water concentration over the coating thickness over time. The model is validated by means of comparing an experimentally measured ORP-EIS capacitance value with a virtual capacitance value, calculated from the predicted local water concentrations. This modelling approach is summarized in Fig. 1. The constraints of the FEM model and ORP-EIS experiments and the discrepancies between the FEM model output and ORP-EIS capacitance validation experiments are described and critically discussed.

2. Experimental

2.1. Materials and sample preparation

Standard steel Q-panels SAE 1008/1010, made from standard low carbon cold rolled steel, were coated with Poly Ethylene Glycol Diacrylate (PEGDA) formulations made by mixing the reagents at 40 °C for at least 12 h. At room temperature, the formulations are spread on the panels using a bar coater to obtain a 100 μm wet film thickness. Upon coating application, the panels are directly placed in a nitrogen purged enclosure and UV-cured with a CF2000 with JL3-400F-90 model LED head lamp, both from Clearstone technologies Inc., having a light power of 16 W and irradiance of 700 mW/cm^2, with an active area of 5 × 4 cm^2 emitting UV light with 400 nm wavelength. This resulted is a dry film thickness of around 60 μm.

2.2. Analysis techniques

2.2.1. Gravimetric analysis

Water uptake was measured by gravimetric analysis on free standing films, produced by peeling of the coating from the steel substrate, with MilliQ water at room temperature using a Metler Toledo MX5 digital microbalance with a precision of 1 μg. The absorbed water mass $X_m(t)$ within the PEGDA coating was calculated using:

$$X_m(t) = \frac{m(t) - m_0}{m_0} = \frac{m_{water}}{m_{adhesive}} \quad (1)$$

with m(t) the mass at each time instance and m_0 the initial mass of the dry sample, for at least three samples for reproducibility reasons.

2.2.2. Attenuated total reflection-Fourier transform infrared spectroscopy (ATR-FTIR)

The presence and molecular configuration of water at the coating/substrate interface was studied using attenuated total reflection-Fourier transform infrared spectroscopy (ATR-FTIR) in Kretschmann geometry using a Thermo-Nicolet Nexus FT-IR spectrometer equipped with a mercury-cadmium-telluride (MCT) liquid-nitrogen-cooled detector in a nitrogen-purged measurement chamber with a VeeMAXIII single reflection ATR accessory. The spectra were recorded from 600 to 5000 cm^{-1} under an angle of 75° with a resolution of 8 cm^{-1}.

The detailed procedure for the sample preparation specifically for ATR-FTIR in Kretschmann geometry can be found elsewhere [15]. Measurements were performed in a 1 M NaSCN aqueous solution as an infrared active pseudo-halide since technically more relevant chloride solutions are inactive in the IR region.

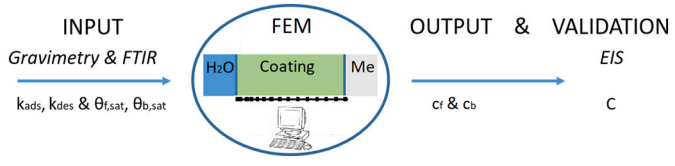

Fig. 1. The modelling approach indicating the relevant techniques, model parameters k_{ads}, k_{des}, $\theta_{f,sat}$ and $\theta_{b,sat}$ and model variables c_f and c_b for the three building blocks.

2.2.3. Odd random phase electrochemical impedance spectroscopy (ORP-EIS)

The electrochemical behaviour of the organic coating in contact with water and the associated coating capacitance was studied over time with odd random phase electrochemical impedance spectroscopy (ORP-EIS). The electrochemical data is obtained using a National Instruments PCI-4461 DAQ card, connected to an in-house built compact analog potentiostat using in-house developed software. An Ag/AgCl reference electrode and a Pt mesh counter electrode were used for all measurements. Different concentrations of a NaCl solution were used as electrolyte. The measurements were started immediately after immersion (30–60 s), starting with an OCP measurement of 10 s. A 10 mV (rms) signal around OCP in the frequency range going from 1 kHz to 5 mHz was imposed and the system was measured repeatedly without waiting time during two consecutive measurements, for at least 2 or 3 samples, to conform their reproducibility. A more detailed description of the technique can be found elsewhere [16,17].

2.3. Finite element modelling

The model was implemented in Comsol Multiphysics version 5.4, a commercially available finite element modelling software, using the transport of diluted species (tds) physics interface. This module studies the evolution of chemical species transported by diffusion and convection, assuming they are dilute and that consequently the mixture properties correspond to those of the solvent. The chemical species transport by diffusion and convection is modelled by solving the mass conservation equation for the different contributing chemical species.

3. Results and discussion

The approach followed to model the water transport through organic coatings consists of three building blocks: the model input, the model itself and the model output and validation. FTIR and gravimetric measurements serve as the input for the model in order to obtain the relevant parameters to build the model together with a number of coating properties such as the coating thickness, density and relative permittivity etc. Impedance measurements serve as the validation tool for the output of the model. Fig. 1 depicts the overview of the modelling approach with the employed techniques and the extracted model parameters and variables. The relevant coating properties can be found in Table 1.

3.1. Finite element model

A one-dimensional (1D) model, capable in following the water uptake along the coating thickness, was built in Comsol Multiphysics using the "Transport of diluted species" interface. This interface models the transport of chemical species through diffusion and convection by solving the mass conservation equation for all diluted chemical species i contributing:

$$\frac{\partial c_i}{\partial t} + \nabla . J_i + u . \nabla c_i = R_i \quad (2)$$

with c_i (mol/m^3) the concentration, J_i (mol/(m^2·s)) the mass flux relative to the mass averaged velocity, u (m/s) the mass averaged velocity vector describing the convective transport and R_i (mol/(m^3·s)) the reaction rate expression of the species, respectively. The preference of a 1D model over a 2D model is justified by the currently existing models in literature and the use of validation technique, which is not capable of measuring lateral diffusion [1,2].

In the case that mass transport is governed only by molecular diffusion, assumed in this model, the convective transport term can be

Table 1
Values of variables and parameters used in this model with their respective standard deviation if applicable for the different coating systems.

Variable	Name	Value	Std	Unit	Ref.
c_f	Free water conc.			mol/m^3	
c_b	Bound water conc.			mol/m^3	
Model parameters					
k_{ads}	Adsorption rate const.	1.15 × 10^{-9}	R^2 = 0.88	m^3/(s·mol)	
k_{des}	Desorption rate const.	2.19 × 10^{-4}	R^2 = 0.76	1/s	
$\theta_{f,sat}$	Saturation conc. free water	247	41	mol/m^3	
$\theta_{b,sat}$	Saturation conc. bound water	352	59	mol/m^3	
Coating properties					
d	Coating thickness (model)	100		µm	
	Coating thickness (validation)	60	9	µm	
D	Diffusion constant	3.9 × 10^{-13}	0.3	m^2/s	[8]
$\varepsilon_{coating}$	Rel. permittivity coating	5.48	0.01		[8]
ρ_c	Coating density	1125		kg/m^3	[26]
[S]	Conc. of available sites	127.34		mol/l	
Constants					
ε_{H2O}	Rel. permittivity water	80			
A	Coating area	1		m^2	

omitted and the mass flux J_i defines the diffusive flux vector:

$$J_i = -D\nabla c \tag{3}$$

with D (m^2/s) the diffusion coefficient.

The right-hand side of Eq. (2), typically representing a source or sink term as a consequence of chemical reaction or desorption on porous matrix, can then be associated with the physical adsorption/desorption reaction of free water $(H_2O)_f$ into bound water $(H_2O)_b$ in the porous coating structure, i.e.:

$$(H_2O)_f + S \rightleftarrows^{k_{ads}}_{k_{des}} (H_2O)_b \tag{4}$$

The adsorption/desorption reaction of adsorbent A on site S is typically represented by [18]:

$$A + S \rightleftarrows AS \tag{5}$$

according to the Langmuir adsorption model. As such, the adsorption r_{ads} (mol/(m^3·s)) and desorption reaction rate r_{ads} (mol/(m^3·s)) expression can be written as:

$$r_{ads} = k_{ads} c_f [S] \tag{6}$$

and

$$r_{des} = k_{des} c_b \tag{7}$$

with k_{ads} (m^3/mol·s) and k_{des} (1/s) the reaction rate constants of the adsorption and desorption reaction, respectively. c_f (mol/m^3) and c_b (mol/m^3) represent the concentration of free and bound (adsorbed) water present in the coating structure, respectively, and [S] represents the number of available sites on the polymer matrix within the coating structure for adsorption expressed as a concentration (in mol/m^3). If we write the maximum number of available sites for free and adsorbed water as $\theta_{f,sat}$ and $\theta_{b,sat}$, respectively, expressed as a concentration (in mol/m^3) rather than a surface coverage in the Langmuir adsorption model, the reaction rate expression in the case of water adsorption/desorption becomes [18]:

$$r_{ads} = k_{ads} c_f \left(\theta_{b,sat} - c_b\right) \tag{8}$$

and

$$r_{des} = k_{des} c_b \tag{9}$$

The overall reaction rate can then be written as:

$$R = r_{ads} - r_{des} \tag{10}$$

which defines the source/sink term in the mass balance equation (Eq. (2)), as explained earlier. Despite the Langmuir adsorption model's strong hypothesis, i.e. assuming adsorption of a perfect monolayer at homogeneous sites, it is selected over empirical model such as the Freundlich adsorption model, and other theoretical models such as the Brunauer–Emmett–Teller (BET) adsorption model and the Temkin adsorption model, because of its (physical) simplicity while keeping the number of model input parameters limited, which are besides easily accessible [19].

The boundary conditions can be derived by supposing chemical equilibrium on the water/coating interface and solving for c_b, imposing that the free water concentration c_f equals the saturation concentration of free water $\theta_{f,sat}$. The initial values for the free and bound water over the coating thickness are set to 1/100 of the saturation concentration, respectively, arbitrarily selected to represent the small amount of water initially present in the 'dry coating' and to avoid computational convergence issues. A graphical representation of the model implementation can be found in Fig. 2.

As such this modelling approach gives rise to four intrinsic model parameters, i.e. the reaction rate constants for the adsorption/desorption reaction (k_{ads} and k_{des}) and the saturation concentrations of free and bound water ($\theta_{f,sat}$ and $\theta_{b,sat}$) (Fig. 1). These will be estimated from FTIR and gravimetric analysis measurements, respectively.

3.2. Estimation relevant model input parameters

3.2.1. FTIR

In-situ infrared spectra were recorded in the first 125 h after exposure to a 1 M NaSCN solution for the PEGDA coating. The evolution of the water peak (OH-stretching vibration, 2900–3800 cm^{-1}) is evaluated over time using the infrared spectrum of the dry adhesive as the reference [15]. For a more detailed interpretation, this peak was fitted according to the four different summative states of water, i.e. monomeric, dimeric, clustered and bulk water, and their respective integrated peak areas [20]. Since the first three are all considered as forms of bound water, their respective integrated peak areas are summed and plotted over time and evaluated versus the bulk water contribution, which is considered as free water (Fig. 3). Since infrared results provide only

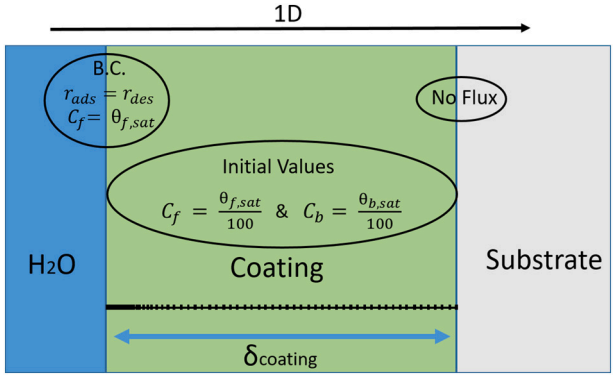

Fig. 2. Implementation of the model in Comsol Multiphysics showing the boundary conditions and initial values used for the simulation of the water uptake as well as the mesh and its nodes used in this model.

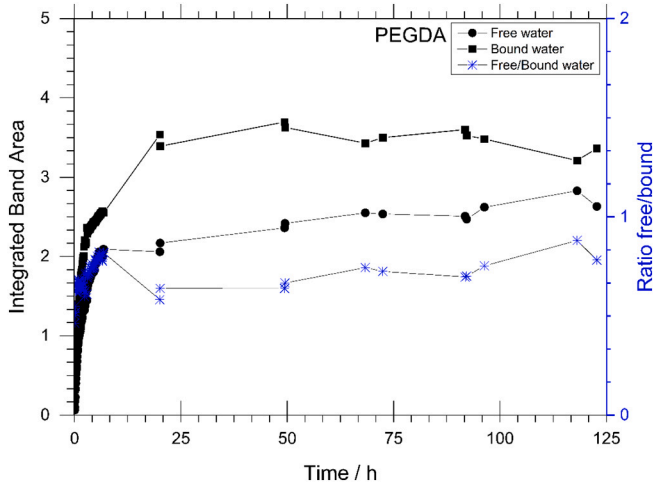

Fig. 3. Evolution of the free and bound water and the ratio of free to bound water over time after peak deconvolution of FTIR results for the PEGDA coating.

qualitative information (quantified concentrations cannot be obtained from the integrated absorbance), the ratio between the integrated peak area of the free states of water and the bound state of water is calculated over time in order to obtain semi-quantitative data. It can be observed (Fig. 3) that the individual contributions of free and bound water rapidly increase over time initially before reaching a stable contribution with a ratio of free water versus bound water of 0.7 for the PEGDA system.

The FTIR information can also be used to estimate the reaction rate constants [21]. The desorption reaction is regarded as a first order reaction in this model and the adsorption reaction can be considered a pseudo- first order reaction since the concentration of water in the polymer is negligible compared to the number of available sites to be adsorbed at. Due to the (pseudo)-first order character, the absorbance values of both the free and bound water peak exhibit an exponential change with reaction time. As such kinetic parameters can be deduced from the exponential fitting of the absorbance difference ΔA, i.e. the difference between the absorbance at a given time instance and the absorbance at equilibrium ($\Delta A = A(t) - A(\infty)$), versus time (Fig. 4) [21].

The resulting (pseudo) first-order constants for the adsorption and desorption reaction are 1.46×10^{-4} 1/s and 2.19×10^{-4} 1/s with respective coefficients of determination (R^2) of 0.88 and 0.76. The latter can directly be used as the estimate for k_{des} while the former has to be divided by the concentration of available sites for adsorption [S], i.e. 127.34 mol/l, estimated from the total number of hydrogen bonding –donor and -acceptor sites available on the respective coating matrix to adsorb water on. This results in an adsorption rate constant (k_{ads}) of 1.53×10^{-9} $m^3/(mol \cdot s)$.

3.2.2. Gravimetrical analysis

The averaged experimental sorption curve with its standard deviation as measured by gravimetry is presented in Fig. 5. It shows a stable mass water uptake of approximately 0.95 wt% after 20 min up to 135 min for the PEGDA coating. Taking into account the respective specific density of the coating (Table 1), this corresponds to a water saturation concentration of 600 $mol \cdot m^{-3}$. In this regard, no distinction is made between absorption through Fickian diffusion in the initial stages and the contribution of polymer swelling afterwards.

Making the approximation that the ratio between the free and bound water concentration, obtained from FTIR measurements previously, is the same over the coating thickness, the saturation concentration for the free ($\theta_{f,sat}$) and bound ($\theta_{b,sat}$) water becomes 247 ± 41 mol/m^3 and 352 ± 59 mol/m^3. This, together with the adsorption and desorption rate constants k_{des} and k_{des}, concludes the list of necessary input parameters

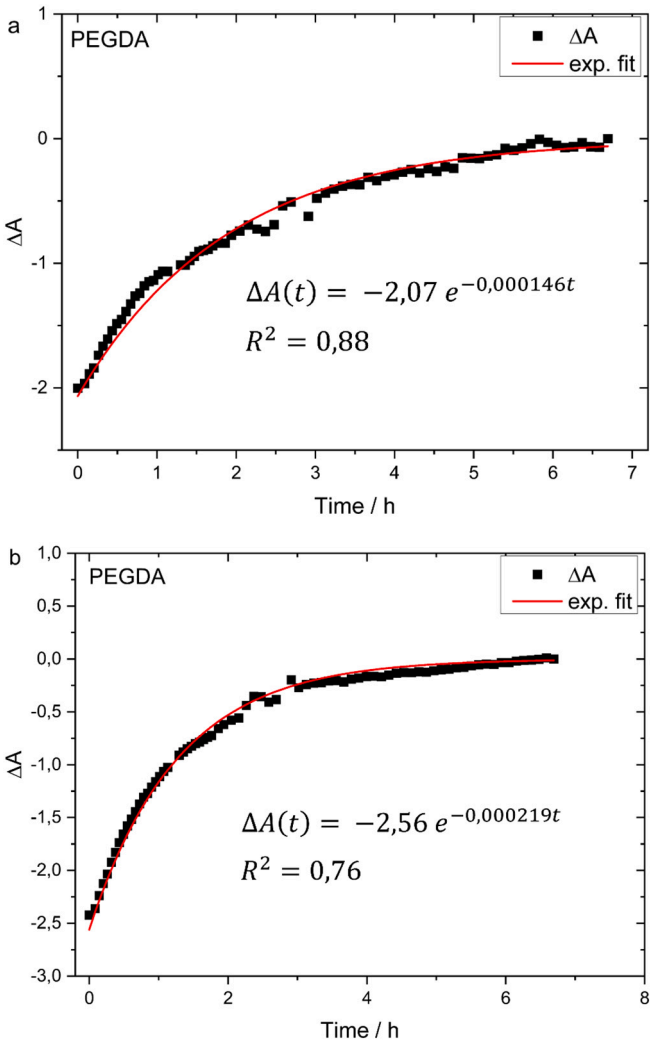

Fig. 4. Absorbance difference ΔA over time and exponential fitting of the FTIR results for the free (a) and bound (b) water to obtain the kinetic rate constant values k_{ads} and k_{des} for the adsorption/desorption reaction of water for the PEGDA coating.

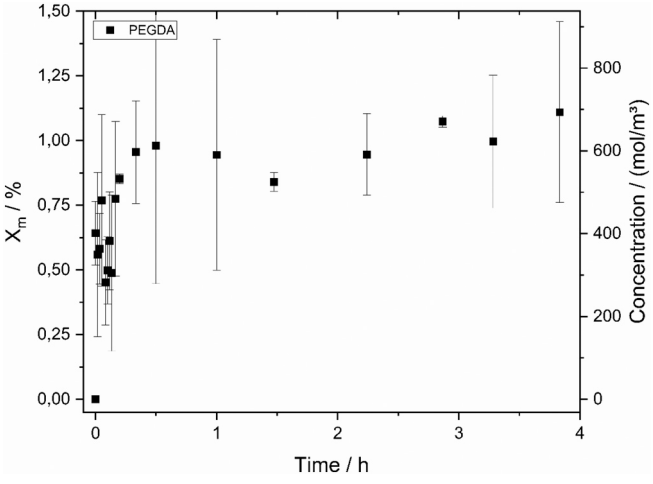

Fig. 5. Gravimetry results showing the mass water uptake X_m (%) and the total water concentration over time with their respective standard deviation for the PEGDA coating.

for the model.

An overview of the values of the relevant coating properties necessary for the model and of the variables and model parameters can be found in Table 1. The diffusion constant D has been obtained from earlier work, where it has been determined from the relationship between volumetric fraction of water and time for the PEGDA coating [6,8].

3.3. Model output

Based on the necessary coating properties and model parameters, listed in Table 1, the 1D model is able to predict the concentration of free and bound water over the coating thickness and over time for a coating thickness of 100 μm (Fig. 6). The evolution of the free water concentration (Fig. 6a) in the first 168 h reveals a rapid increase in the initial hours before reaching the coating water saturation concentration value ($\theta_{f,sat}$) over the coating thickness after 16 h, corresponding to 247 mol·m^{-3}. A more gradual increase is seen for the bound water concentration (Fig. 6b) compared to the free water concentration, associated with adsorption kinetics rather than diffusion kinetics, respectively. Nevertheless, the bound water concentration reaches a stable value over the coating thickness of less than 1 mol·m^{-3} after 16 h, substantially lower than the expected saturation value of 352 mol·m^{-3} estimated by means of gravimetric and FTIR measurements before.

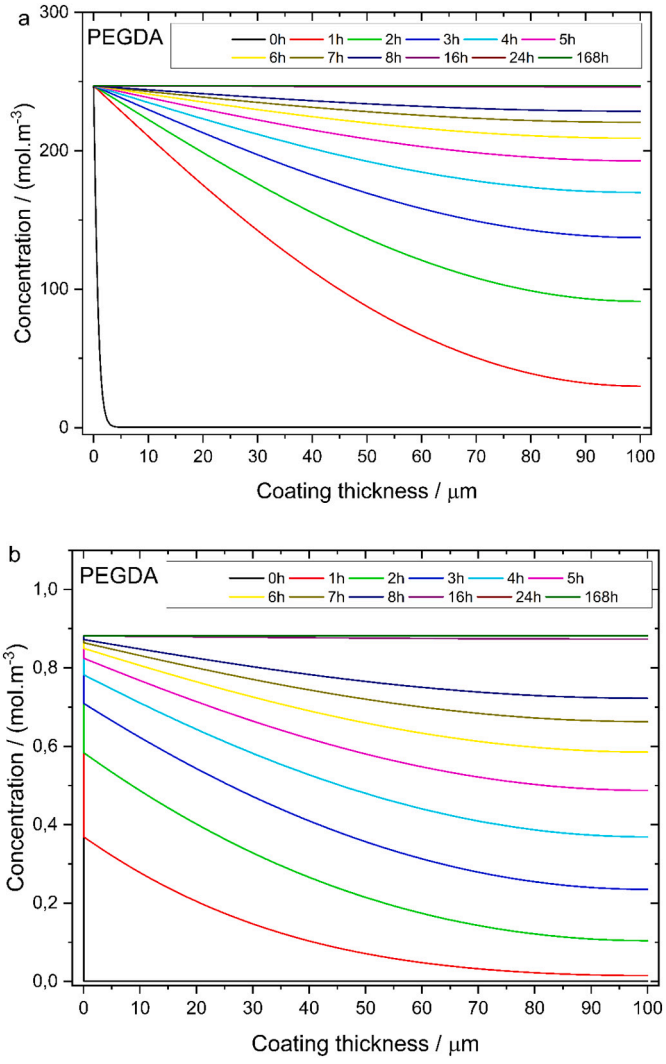

Fig. 6. Modelled concentration of free (a) and bound (b) water over the coating thickness as a function of time for the PEGDA system for a model coating thickness of 100 μm.

3.4. Model validation with impedance measurements

At this stage, the challenge comes to light whether the predicted water uptake profiles can be validated in a reliable way with experimental water uptake profiles. Validation of the water concentration profiles is strictly necessary in order to use them as a correct starting point for modelling of the associated interfacial electrochemistry and coating delamination at a later stage. Therefore, independent odd random phase electrochemical impedance spectroscopy (ORP-EIS) measurements are carried out, allowing instantaneous and reliable monitoring of the impedance behaviour of organic coatings during water uptake by applying a broadband rather than a single sine signal, allowing determination of the standard deviation on the measured impedance points [16,22].

Starting from the concentration of free and bound water as a function of coating thickness and over time, as resulting from the FEM model, the overall capacitance of the coating system is calculated. Therefore, the local total water concentration is calculated at every point over the thickness of the coating (or every mesh node in the 1D FEM model (Fig. 2)) by summing the free and bound water concentration. For each local water concentration, the effect on the local permittivity of the system can be calculated through effective medium approximations using the Maxwell-Garnett equation:

$$\left(\frac{\varepsilon_{eff}-\varepsilon_m}{\varepsilon_{eff}+2\varepsilon_m}\right)=\delta_i\left(\frac{\varepsilon_i-\varepsilon_m}{\varepsilon_i+2\varepsilon_m}\right) \tag{11}$$

with ε_{eff} the effective permittivity of the system, ε_i the permittivity of the inclusions (water) and ε_m the permittivity of the medium (coating) and δ_i the volume fraction of the inclusions [23]. This local effective permittivity is subsequently translated in a local capacitance C (F/m^2) according to the capacitor's definition:

$$C=\frac{\varepsilon_{eff}\varepsilon_0 S}{d} \tag{12}$$

with ε_{eff} the effective permittivity of the system as calculated using the Maxwell-Garnett equation, ε_0 (F/m) vacuum permittivity, S (m^2) the coating area and d (m) the coating thickness [24]. Finally these local capacitances distributed along the coating thickness in series are summed according to the capacitances in series rule, i.e. summing the reciprocal of the individual capacitances, in order to obtain the overall coating capacitance. These 'virtual' capacitance values can then be compared against the experimentally measured impedance data after extraction of the experimental capacitance values.

Fig. 7 shows the Bode plots for the PEGDA coating after 20 min; 1.5 h; 3 h; and 51 h of immersion, respectively, as measured by ORP-EIS in a 0.05 M NaCl solution. The black line and the grey line correspond to the magnitude of the impedance modulus and the phase angle, respectively, as usually plotted by classical EIS. The other characteristics of the experimental data of an ORP-EIS measurement are provided by the curves representing the noise (blue), the noise plus the non-linearities (red) and the noise plus the non-stationarities (green) [16,25]. From the result after 20 min (Fig. 7a) it can be seen that, right at the start, the noise + non-linearities curve is not overlapping the noise curve, indicating non-stationary behaviour. This mismatch is especially apparent at high frequencies, but decreases after longer times (Fig. 7b and c). These non-stationarities observed at the higher frequencies suggest that the electrochemical processes with low characteristic time constants (fast processes) mainly cause the time-variant behaviour of the system [8]. This can be related to the non-stationary water uptake of the PEGDA coating. Moreover, it can be observed that the magnitude of the impedance modulus lies around 10^6 Ω·cm^2 and 10^{10} Ω·cm^2 at the highest and lowest frequencies measured, i.e. 1 kHz and 5 mHz, respectively.

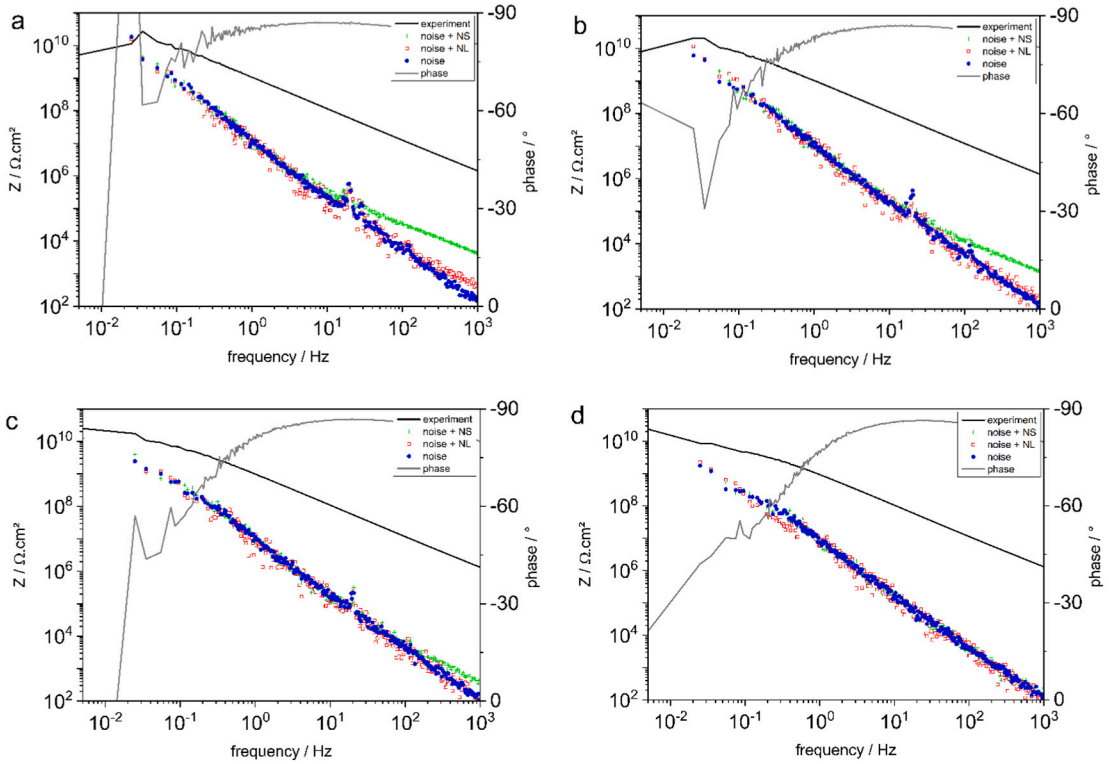

Fig. 7. ORP-EIS spectra of the PEGDA coating during water uptake recorded after 20 min (a), 1.5 h (b), 3 h (c) and 51 h (d) showing the magnitude of the impedance, the phase angle and the contribution of the noise, non-linearities and non-stationarities on the measurement.

The experimental capacitance values are obtained from the real Re (Z) and imaginary Im(Z) part of the impedance at a frequency of 1 kHz, justified by the purely capacitive behaviour (phase angle −90°) (Fig. 7) [24]:

$$C = \frac{-Im(Z)}{2\pi f\left(Re(Z)^2 + Im(Z)^2\right)} \tag{13}$$

without fitting the impedance data to an EEC, in order not to introduce fitting errors in the validation study. Fig. 8 shows the modelled capacitance values, based not only on Fickian diffusion but also taking into account the water adsorption/desorption reaction on the polymer, and the experimental capacitance values, extracted from ORP-EIS measurements on PEGDA coatings with a thickness of 60 ± 9 μm, in the first 60 h after exposure of the coating to water. Since coating capacitance is dependent on coating thickness, it is importance that the model thickness and experimental thickness are in agreement. It can be seen for the PEGDA coating that the experimental capacitance values are approximately 4 times higher and shows a different trend in the early stages, with a faster increase in capacitance value, compared to the modelled 'virtual' capacitance values. Therefore, the change in capacitance value over time (ΔC) is considered for comparison purposes, rather than the capacitance value itself. It can be observed that the modelled 'virtual' capacitance value increases by only 1 %, compared to a 15 % increase for the experimental capacitance value.

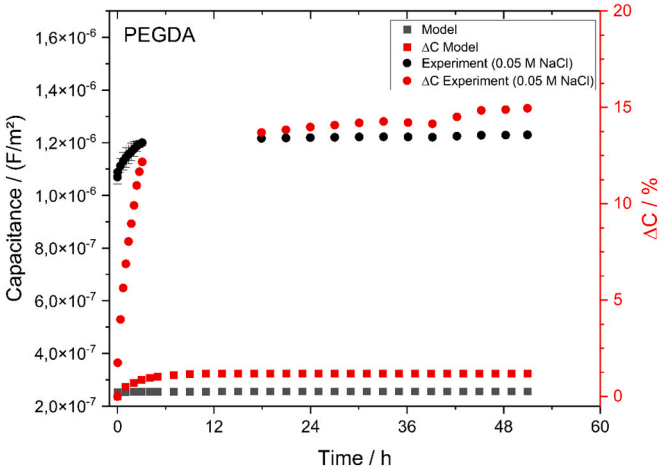

Fig. 8. FEM capacitance values and experimental capacitance values measured in 0.05 M NaCl over time for the PEGDA coating with their respective standard deviation. The red graphs present the respective capacitance difference ΔC over time. (For interpretation of the references to colour in this figure legend, the reader is referred to the web version of this article.)

It needs to be remarked that, since the initial capacitance value is dependent on the permittivity of the dry coating, the trend in terms of the capacitance variation over time provides a more accurate measure to validate the finite element model.

The question remains to what extent we can reliably validate the FEM model with experimentally obtained capacitance values. Therefore, the constraints of the FEM model and ORP-EIS experiments and the differences and discrepancies between the FEM model output and ORP-EIS capacitance validation experiments are listed and critically discussed leading to model improvements, eventually.

3.5. Critical appraisal of the model validation

Apart from the unavoidable standard deviation on either the fitted model parameters on the input side such as the diffusion constant, the reaction rate constants and the saturation concentrations determined by FTIR or gravimetric analysis (which are not determined in this work) or the standard deviation on the extracted capacitance values from EIS and interpretation on the validation side, there are some explicit differences between which phenomena are included in the model and all effects

occurring during the experimental verification. The objective of this part is to identify and critically discuss the major factors on the input, model and validation side separately that account for the discrepancies between the model outcome and the experimental validation and to propose possible model improvements and a more reliable validation.

3.5.1. Validation approach and related approximations

The followed verification approach includes comparison of the experimental capacitance value extracted from an EIS measurement at 1 kHz with a 'virtual' capacitance value after recalculation of the model's output local concentrations into local effective permittivities using the Maxwell-Garnett approximation and finally into local capacitances and an overall capacitance value. To identify the influence of this approximation, another verification approach is followed by comparing directly the model's output overall concentration with the water concentration calculated from the EIS measurements. Therefore the volumetric water uptake $\Phi_{w,v}$ (%) is calculated from the fitted capacitance value at 1 kHz using a linear (Eq. (14)) or Brasher-Kingsbury (B-K, Eq. (15)) approach [8] as a function of the permittivity calculated from the fitted capacitance value at 1 kHz (ε), the permittivity of the dry coating (ε_c) and the permittivity of water (ε_w):

$$\Phi_{w,v} = \frac{\varepsilon - \varepsilon_c}{\varepsilon_w - \varepsilon_c} \tag{14}$$

$$\Phi_{w,v} = \frac{log\frac{\varepsilon}{\varepsilon_c}}{log\varepsilon_w} \tag{15}$$

The volumetric water uptake is then converted in the mass water uptake and finally recalculated into a water concentration. As such, the comparison can be carried out in terms of concentration rather than capacitance, avoiding the use of the Maxwell-Garnett approximation. Also, since the determination of the volumetric water content through the linear approach (Eq. (14)) is based on the difference in permittivity between the wetted coating and the initial dry coating permittivity at all times, it intrinsically uses the change in permittivity, i.e. the trend, similarly to the change in capacitance (ΔC) that was calculated from the capacitance values to study the trend of the results. This results also in having all possibly introduced errors from approximations and approaches on the same side, i.e. the experimental side, while no recalculations are done on the model side. Moreover, recalculation of the experimentally obtained capacitance values into concentrations intrinsically normalizes for the coating thickness through the calculation of the coating permittivity. This allows the comparison of coatings with notable different coating thickness and a reliable calculation of the errors on the obtained water concentration values.

Moreover, the comparison of total water concentration between model and validation also allows us to include the total water concentration as measured by gravimetrical analysis and as such also evaluate the difference between model input, model output and model validation (Fig. 9). It can be seen that for the PEGDA coating, both the linear and the B-K approach are overestimating the total water concentration. Also the gravimetry input concentration values are significantly higher compared to the model outcome. The difference in water uptake between gravimetric and EIS measurements and more precisely the overestimation in water uptake by the linear and B-K approach can be explained in terms of swelling, since these approaches are not taking into account polymer swelling [24].

Since three different approximations/approaches are used for the validation of the modelling results (i.e. Maxwell-Garnett approximation, linear approach and B-K approach) it is important to evaluate the impact that is made on the results by applying each of them. Therefore, from the model outcome for the PEGDA coating, i.e. the total water concentration over time, the capacitance value over time is calculated using the Maxwell-Garnett approximation and recalculated back into a concentration value using the linear approach and the B-K approach in parallel. Doing so, no experimental data is considered, which allows us to

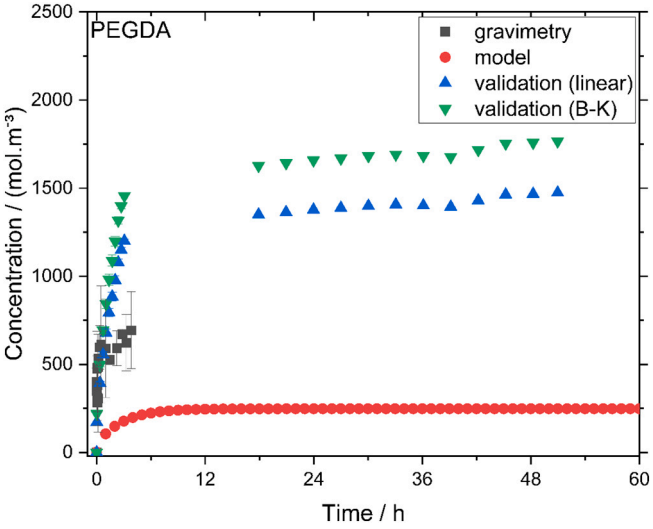

Fig. 9. Comparison of the gravimetry input, model output and validation water concentration values measured in 0.05 M NaCl with their respective standard deviation for the PEGDA coating.

evaluate the difference between the starting concentration value and the final concentration values introduced by the approaches/approximations without bringing measurement errors in the discussion. It can be seen that the final obtained concentrations through both recalculations are substantially lower compared to the starting concentration (Fig. 10), with the B-K approach and the linear approach resulting in approximately 60 % and 10 % of the initial concentration, respectively.

This together with the previous observations regarding the approximations/approaches shows the importance of considering the errors that are made using approximations/approaches in order to validate any model in a reliable way, which is often overlooked.

3.5.2. Measurement parameters of validation experiments

Another difference between the model and the validation experiment is the presence of ions, i.e. in the model no ions are considered while the use of ions for impedance measurements is strictly necessary. To

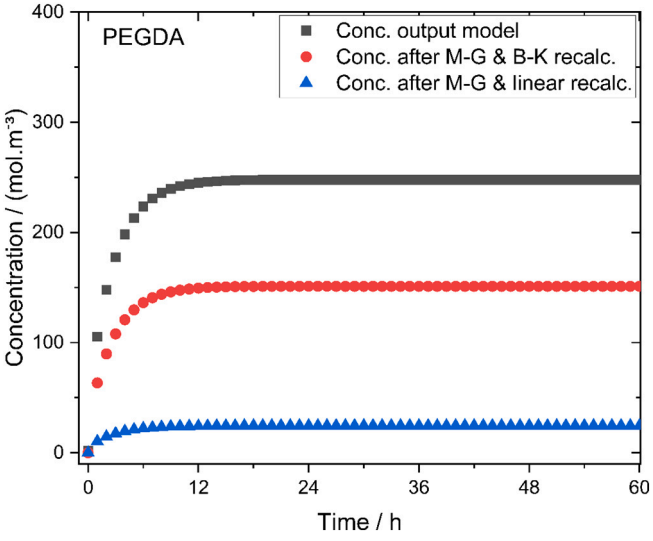

Fig. 10. Comparison of the total water concentration value obtained as output directly from the model with the concentration values obtained from recalculating the model output concentration value into a capacitance value using the Maxwell-Garnett approximation and back into a concentration using the linear and Brasher-Kingsbury approach, respectively, for the PEGDA coating.

estimate the influence of the presence of ions during the ORP-EIS measurement and moreover the importance of their concentration, repetitious impedance measurements are carried out for the PEGDA system while lowering the concentration to virtual zero concentration, which compares to the FEM model situation (Fig. 11). It can be seen that (Fig. 11a) lowering the NaCl concentration from 50 mM to 0.5 mM reduces the capacitance value from 1.2 $\mu F \cdot m^{-2}$ to 0.6 $\mu F \cdot m^{-2}$ which is in better agreement with the 0.25 $\mu F \cdot m^{-2}$ the model (without ions) is predicting. The effect of ions on the water uptake can consequently not be overlooked and influences our interpretation of the water uptake based on the coating capacitance [15]. Re-evaluating the experimental conditions for the model input experiments based on this observation, it can be noticed that water uptake of the gravimetric experiments is not influenced since MilliQ water is used and that the water uptake during FTIR analysis is possibly influenced by the use of NaSCN ions. Nevertheless, since no quantitative information is extracted there, studying the influence of the use of NaSCN ions on the water uptake is out of the scope of this research.

Here again, the comparison can be carried out in terms of concentration rather than capacitance, avoiding the use of the Maxwell-Garnett approximation. It can be seen that (Fig. 11b) by lowering the NaCl concentration the extracted water concentration values are also in better agreement with the model outcome. Moreover, the lower NaCl concentrations are particularly better in agreement with the model outcome if we evaluate them in terms of concentration rather than capacitance, and in particular the linear approach. Therefore, together with earlier observations regarding the use of concentrations for validation purposes, the model validation will be carried out in terms of concentrations rather than capacitances from now on.

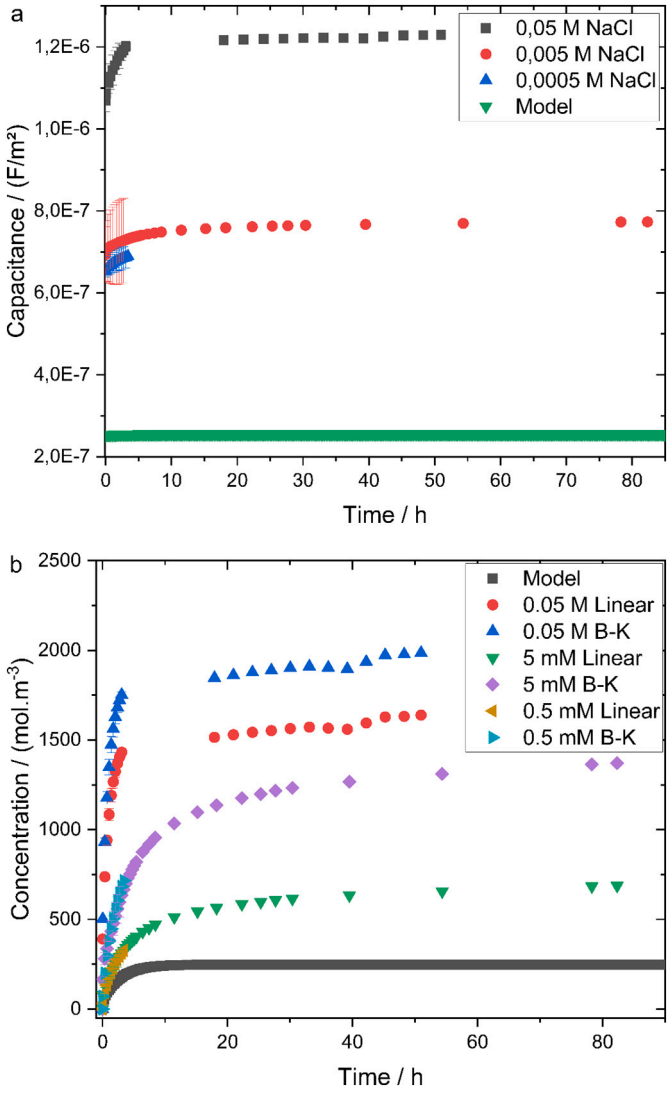

Fig. 11. Effect of NaCl concentration during EIS measurement on the extracted capacitance (a) and water concentration (b) values and comparison with the model output.

It can be concluded here that the presence of ions and their concentration is of high importance and affects the uptake of water in coatings [8,15]. Consequently the way EIS results are interpreted is influencing our interpretation of the water uptake and as such also the validation of the FEM model.

3.5.3. Polymer swelling

Polymer swelling is theoretically estimated according to the volumetric swelling ratio calculated from the gravimetric analysis results [25]:

$$volumetric\ swelling\ ratio = \frac{V_s - V_i}{V_i}$$

where V_s and V_i represent the polymer volume during water uptake and the initial polymer volume, respectively. From the weight mass increase during polymer swelling and taking into account the density of the coating and water, the volumetric swelling ratio is roughly estimated around 1.11 %. Polymer swelling, physically occurring in the polymer coating during water uptake, causes a discrepancy between the interpretation of gravimetric analysis and EIS results as mentioned before. Taking it into consideration would also contribute to a better representation of the real physical situation. In a first step to account for polymer swelling in the finite element model, 1 % theoretical swelling is considered, in order to evaluate the influence of taking polymer swelling into account.

Conceptually, we consider the extra coating volume generated by this thickness increase as an extra hydrophilic volume, totally available for water uptake. As such, 555.6 $mol \cdot m^{-3}$ water extra can be absorbed by the coating (corresponding to 1 % of the free water concentration of 55.5 M), and consequently the maximum saturation concentration $\theta_{max,sat}$ increases from 600 $mol \cdot m^{-3}$ to 1155.6 $mol \cdot m^{-3}$. Taking into account the FTIR ratio of free to bound water of 0.7, the saturation concentrations of free water $\theta_{f,sat}$ and bound water $\theta_{b,sat}$ become 475 $mol \cdot m^{-3}$ and 680 $mol \cdot m^{-3}$, respectively. For modelling purposes, it is assumed that the polymer swelling and the increase in the modelling parameters $\theta_{f,sat}$ and $\theta_{b,sat}$ is linear.

In order to discuss the effect of swelling on the model outcome, the recalculated virtual capacitance values are validated with the 5 mM NaCl EIS measurements (Fig. 12). These are selected over the 0.5 mM NaCl measurements, since the latter was only monitored in the first 5 h and since comparable water concentration values were obtained in this time frame anyway (Fig. 11b), although a lower ion concentration in experimental studies shows better agreement with the finite element model. It can be seen that (Fig. 12) the water concentration profile taking into account polymer swelling is in better agreement with the experimental water profiles compared to the water concentration profile without considering swelling. Taking into account more physical effects in the model gives rise to a more reliable model validation.

3.5.4. Hypothesis model parameters

In order to define the model parameters $\theta_{f,sat}$ and $\theta_{b,sat}$, FTIR and gravimetric analysis measurements were used, i.e. the ratio between the free and bound water molecules was used to divide the maximum water uptake in the free and bound water saturation concentration. However, this is considered as a drastic hypothesis since the FTIR ratio is measured at the coating/metal interface and maximum water uptake reflects the water uptake averaged over the entire coating thickness. To determine the impact of this hypothesis, the use of the FTIR ratio is cancelled out

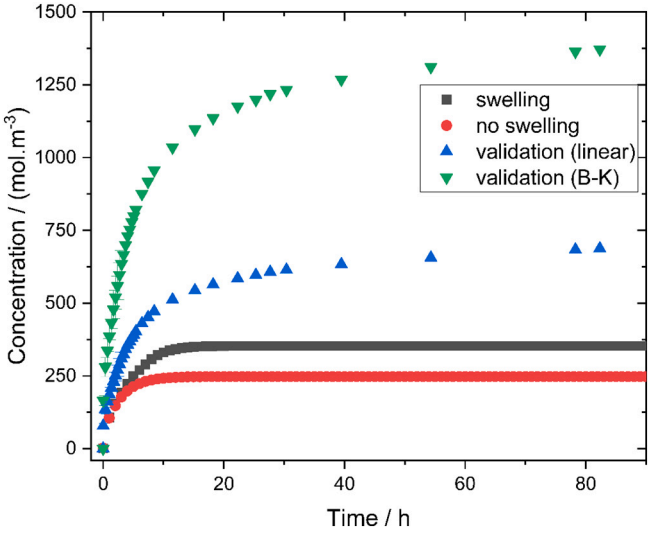

Fig. 12. Water concentration values of the model with and without taking into account polymer swelling, and experimental validation (linear and B-K approach) with 5 mM NaCl for the PEGDA coating.

and only the maximum water uptake is used. Therefore, $\theta_{f,sat}$ and $\theta_{b,sat}$ are no longer constants in this model but become 'dynamic variables' dependent on the instantaneous concentrations of free and bound water c_f and c_b, and the maximum saturation concentration $\theta_{max,sat}$:

$$\theta_{f,sat} = \theta_{max,sat} - c_b \tag{16}$$

$$\theta_{b,sat} = \theta_{max,sat} - c_f \tag{17}$$

The maximum saturation concentration $\theta_{max,sat}$ taken is equal to saturation concentration as measured by gravimetric analysis and is equal to 600 mol·cm^{-3}. Fig. 13 shows the evolution of the concentration over the coating thickness as a function of time. It can be seen that (Fig. 13a) the concentration of free water increases over time, reaching a maximum after around 8 h of around 550 mol·cm^{-3}, close to the maximum saturation concentration. From the concentration of bound water (Fig. 13b) it can be seen that the concentration increases strongly in the first hour indicating a lot of water is adsorbed, before gradually decreasing again. Overall the total water concentration (Fig. 13c), reflecting the behaviour of the sum of the free and bound water, indicates that the PEGDA coating adsorbs approximately 550 mol·m^{-3} in the first 8 h, close to its maximum saturation concentration value. Compared to the initial hypothesis, the uptake of water has increased, since the FTIR ratio is not governing the free and bound water concentration anymore but only the maximum saturation concentration is implied. It can be observed that the free water concentration becomes dominant now and its concentration is substantially higher than in the scenario of the initial hypothesis (Fig. 6e). The concentration of bound water is comparable for both hypotheses (Figs. 13b and 6f),

Yet again, in order to interpret the consequences of this new hypothesis regarding the saturation concentration of free and bound water by considering them as dynamic variables rather than model parameters, the model output concentration following the new and initial hypothesis are compared and validated against a 5 mM NaCl measurement by comparing both water concentration profiles (Fig. 14). It can be seen that the water concentration profile for the new hypothesis is in much better agreement with the experimental water concentration profile (linear approach) compared to the water concentration profile for the old hypothesis. Yet again, the linear approach shows better agreement than the B-K approach. It can be concluded that the adapted, more realistic hypothesis allows a more reliable validation of the model with impedance experiments.

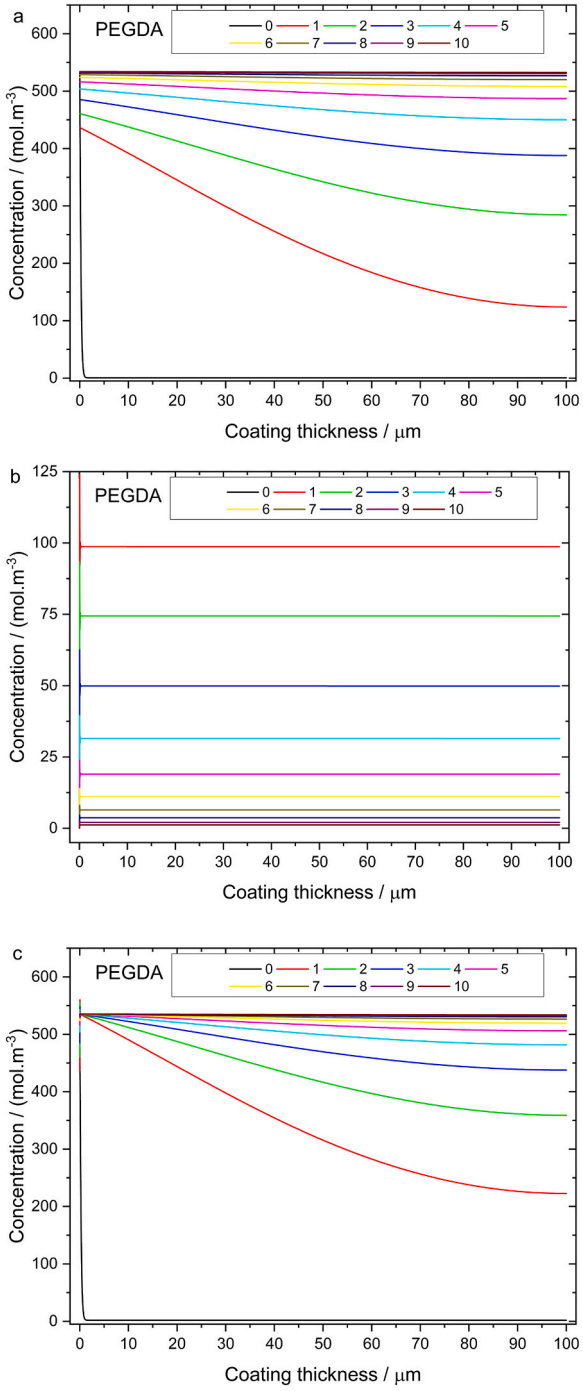

Fig. 13. Effect of the adapted hypothesis for the saturation concentration model parameters $\theta_{f,sat}$ and $\theta_{b,sat}$ on the model output for the PEGDA coating showing the free water concentration (a), the bound water concentration (b) and the total water concentration (c) evolution over the coating thickness in the first 10 h for a model coating thickness of 100 µm.

3.5.5. *Combined effect of polymer swelling and adapted hypothesis*

Finally, both the effect of polymer swelling and the adapted hypothesis are incorporated in the model in order to study the impact on the model outcome and the virtual capacitance values. These effect, discussed in paragraph 3.5.3 and 3.5.4 already, cause the $\theta_{max,sat}$ to increase to 1155 mol·m^{-3} and do not take the FTIR ratio into account anymore by considering $\theta_{f,sat}$ and $\theta_{f,sat}$ as dynamic variables and no longer as fixed model parameters. In Fig. 15, the obtained water concentration profile taking into account both model adaptions is compared

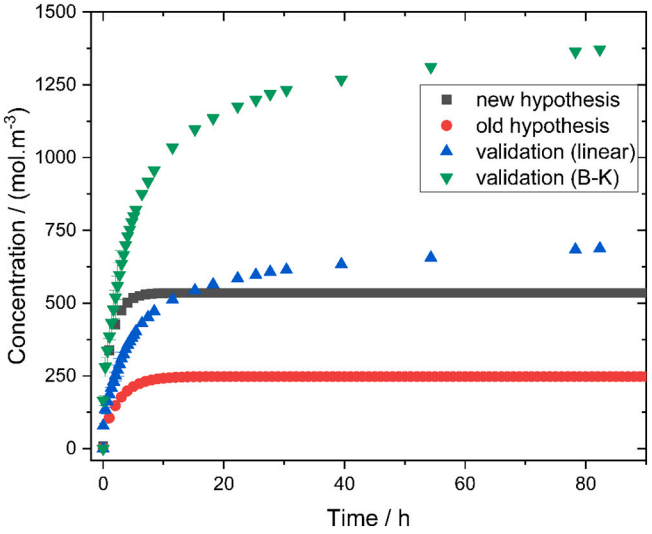

Fig. 14. Water concentration values of the model for the new and old hypothesis regarding the saturation concentration parameters $\theta_{f,sat}$ and $\theta_{b,sat}$, and experimental validation (linear and B-K approach) with 5 mM NaCl for the PEGDA coating.

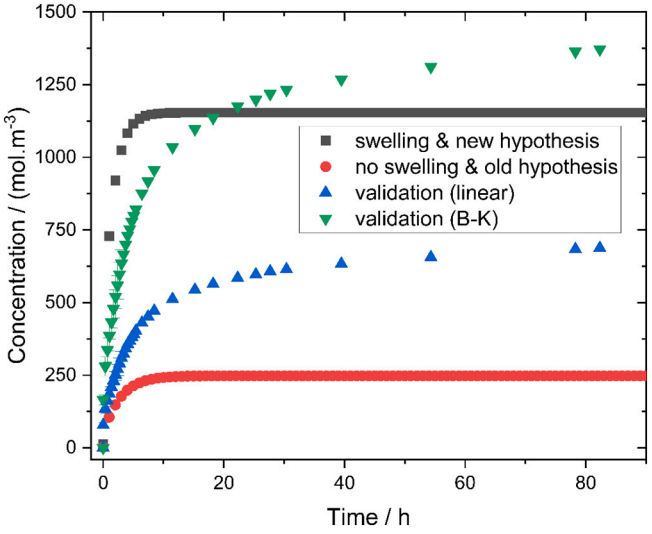

Fig. 15. Water concentration values of the model taking into account both polymer swelling and the adapted hypothesis, and experimental validation (linear and B-K approach) with 5 mM NaCl for the PEGDA coating.

with the water concentration profile without model adaptions and evaluated versus the experimentally obtained water concentration profiles for 5 mM NaCl. It can be seen that taking into account the combined effect of polymer swelling and the adapted hypothesis causes the water concentration profile to increase strongly compared to the water concentration profile without considering them. Compared to the gravimetric water uptake after 4 h, taking into account polymer swelling, and reaching a water concentration of around 750 mol·m^{-3} (Figs. 5 and 9), the modified model predicts a total water concentration of around 1000 mol·m^{-3} after 4 h. Moreover, the obtained water concentration profile is in much better agreement with the experimentally obtained water concentration profiles. Note that the impact of taking both model improvements into account is stronger than considering the polymer swelling and new hypothesis individually, as can be observed from Figs. 13 and 14.

It can be concluded that by considering both model adaptations a better agreement is found between the predicted water concentration profiles and the validation experiments while contemplating a better physical description of what happens during water uptake in organic coatings. Therefore these model adaptations can be looked at as model improvements resulting in a more reliable model that can successfully be validated by impedance measurements.

Predicting water uptake in organic coatings is merely a first step towards a model capable of predicting long-term durability (under accelerated conditions) and life-time assessment if also the transport of ions and its electrochemistry and delamination could be taken into account in the future.

4. Conclusions

Starting from relevant coating properties as well as gravimetric and FTIR measurements providing information about the water uptake of the coating and the presence of free and bound water at the coating interface water uptake through an organic coating is modelled by solving the mass conservation equation taking into account Fickian diffusion and the water adsorption/desorption reaction on the coating structure. The model is able to predict the water concentration profile over the thickness of the coating over time. The key aspect of this approach is the experimental validation of the developed water uptake model and to what extent this can be performed. Therefore, virtual EIS capacitance values are calculated from the water concentration profiles and compared with experimental capacitance values obtained from impedance measurements. In parallel, from the experimental capacitance values also water concentration profiles are calculated in order to carry out a validation in terms of concentration rather than capacitance, using different approximations and approaches, allowing the evaluation of their impact on the recalculated values. It has been pointed out that there are several advantages by validation in terms of water concentration profiles rather than capacitance values.

In order to evaluate in detail whether we can reliably validate the model with impedance measurements, the discrepancies between model outcome and validation experiment are critically discussed. These include, apart from the standard deviation on the fitted model parameter estimates (the kinetic rate constants of the adsorption/desorption reaction and the saturation concentrations of free and bound water), the approximations and approaches to compare the model output and the validation results, the physical phenomena occurring such as polymer swelling, and the assumptions/hypotheses that are made building the model. The impact of taking into account these effects on the predicted water concentration profiles over time is discussed individually and it has been exhibited that the impact of these aspects on the model are important to consider. Finally the combined impact of polymer swelling and an adapted hypothesis contemplate not only a better description of what physically happens during water uptake in organic coatings and as such a more reliable model. Therefore these model adaptations can be looked at as model improvements leading to a more reliable validation by impedance measurements.

CRediT authorship contribution statement

M. Meeusen: Conceptualization, Methodology, Validation, Investigation, Writing – original draft, Writing – review & editing. **J.P.B. van Dam:** Investigation. **N. Madelat:** Investigation. **E. Jalilian:** Investigation. **B. Wouters:** Investigation. **T. Hauffman:** Conceptualization, Supervision. **G. Van Assche:** Conceptualization, Supervision. **J.M.C. Mol:** Conceptualization, Supervision. **A. Hubin:** Conceptualization, Supervision. **H. Terryn:** Conceptualization, Supervision, Funding acquisition.

Declaration of competing interest

The authors declare that they have no known competing financial interests or personal relationships that could have appeared to influence the work reported in this paper.

Data availability

Data will be made available on request.

Acknowledgement

This research is funded by the SBO project PredictCor (project number: FWOSBO22) of the Research Foundation – Flanders (FWO).

References

[1] V. Baukh, H.P. Huinink, O.C.G. Adan, S.J.F. Erich, L.G.J. Van Der Ven, Predicting water transport in multilayer coatings, Polymer 53 (15) (2019) 3304–3312.
[2] K.N. Allahar, B.R. Hinderliter, D.E. Tallman, G.P. Bierwagen, Water transport in multilayer organic coatings, J. Electrochem. Soc. 155 (8) (2008) 201–208.
[3] Z. Manoli, D. Pecko, G. Van Assche, J. Stiens, A. Pourkazemi, H. Terryn, Transport of Electrolyte in Organic Coatings on Metal, in: Paint and Coatings Industry, Intech, 2019.
[4] A. Son, N. Causse, M. Musiani, M.E. Orazem, N. Pébère, B. Tribollet, V. Vivier, Determination of water uptake in organic coatings deposited on 2024 aluminium alloy : comparison between impedance measurements and gravimetry, Prog. Org. Coat. 112 (June) (2017) 93–100.
[5] S. Shreepathi, S.M. Naik, M.R. Vattipalli, Water Transportation Through Organic Coatings: Correlation Between Electrochemical Impedance Measurements, Gravimetry, and Water Vapor Permeability 9(4), 2012, pp. 411–422.
[6] E. Jalilian, H. Terryn, G. Van Assche, Water permeation in coatings, J. Coat. Technol. Res. (2020) 1437–1445.
[7] J.H. Park, G.D. Lee, H. Ooshige, A. Nishikata, T. Tsuru, Monitoring of water uptake in organic coatings under cyclic wet – dry condition, Corros. Sci. 45 (2003) 1881–1894.
[8] B. Wouters, E. Jalilian, R. Claessens, N. Madelat, T. Hauffman, G. van Assche, H. Terryn, A. Hubin, Monitoring initial contact of UV-cured organic coatings with aqueous solutions using odd random phase multisine electrochemical impedance spectroscopy, Corros. Sci. 190 (2021), 109713.
[9] J. Rault, The state of water in swollen polymers, Macromol. Symp. 100 (1995) 31–38.
[10] M. Autengruber, M. Lukacevic, J. Füssl, Finite-element-based moisture transport model for wood including free water above the fiber saturation point, Int. J. Heat Mass Transf. 161 (2020), 120228.
[11] X. Fan, V. Nagaraj, Finite Element Modeling of Anomalous Moisture Diffusion With Dual Stage Model, in: IEEE 62nd Electronic Components and Technology Conference, 1192, 2012.
[12] V. Baukh, H.P. Huinink, O.C.G. Adan, S.J.F. Erich, L.G.J. van der Ven, Water-polymer interaction during water uptake, Macromolecules 44 (12) (2011) 4863–4871.
[13] H.G. Carter, K.G. Kibler, Langmuir-type model for anomalous moisture diffusion in composite resins, J. Compos. Mater. 12 (2) (1978) 118–131.
[14] J.M. Arroyave, M. Avena, Determining rate coefficients for ion adsorption at the solid/water interface: better from desorption rate than from adsorption rate, Phys. Chem. Chem. Phys. 22 (20) (2020) 11695–11703.
[15] N. Madelat, B. Wouters, E. Jalilian, G. Van Assche, A. Hubin, H. Terryn, T. Hauffman, Differentiating between the diffusion of water and ions from aqueous electrolytes in organic coatings using an integrated spectro-electrochemical technique, Corros. Sci. 212 (2023), 110919.
[16] Y. van Ingelgem, E. Tourwé, O. Blajiev, R. Pintelon, A. Hubin, Advantages of odd random phase multisine electrochemical impedance measurements, Electroanalysis 21 (6) (2009) 730–739.
[17] T. Breugelmans, J. Lataire, T. Muselle, E. Tourwé, R. Pintelon, A. Hubin, Odd random phase multisine electrochemical impedance spectroscopy to quantify a non-stationary behaviour: theory and validation by calculating an instantaneous impedance value, Electrochim. Acta 76 (2012) 375–382.
[18] M. Misono, Basis of heterogeneous catalysis. Heterogeneous catalysis of mixed oxides, Stud. Surf. Sci. Catal. 1 (176) (2013).
[19] M. Musah, Y. Azeh, J. Mathew, M. Umar, Z. Abdulhamid, A. Muhammad, Adsorption kinetics and isotherm models: a review, Caliphate J. Sci. Technol. 4 (1) (2022) 20–26.
[20] T. Lindfors, FTIR-ATR study of water uptake and diffusion through ion-selective membranes based on plasticized poly (vinyl chloride), Electroanalysis 21 (2009) 1914–1922.
[21] J.E. Roberts, G. Zeng, M.K. Maron, M. Mach, I. Dwebi, Y. Liu, Measuring heterogeneous reaction rates with ATR-FTIR spectroscopy to evaluate chemical fates in an atmospheric environment: a physical chemistry and environmental chemistry laboratory experiment, J. Chem. Educ. 93 (2016) 733–737.
[22] T. Breugelmans, E. Tourwé, J.B. Jorcin, A. Alvarez-Pampliega, B. Geboes, H. Terryn, A. Hubin, Odd random phase multisine EIS for organic coating analysis, Prog. Org. Coat. 69 (2010) 215–218.
[23] V.A. Markel, Introduction to the Maxwell Garnett approximation : tutorial, J. Opt. Soc. Am. 33 (7) (2016) 1244–1256.
[24] C. Vosgien Lacombre, G. Bouvet, D. Trinh, S. Mallarino, S. Touzain, Water uptake in free films and coatings using the Brasher and Kingsbury equation: a possible explanation of the different values obtained by electrochemical impedance spectroscopy and gravimetry, Electrochim. Acta 231 (2017) 162–170.
[25] X. Yang, B.L. Dargaville, D.W. Hutmacher, Elucidating the molecular mechanisms for the interaction of water with polyethylene glycol-based hydrogels: influence of ionic strength and gel network structure, Polymers 13 (6) (2021).
[26] J.M. Vuksanović, M.L. Kijevčanin, I.R. Radović, Poly(ethylene glycol) diacrylate as a novel chaotropic compound for design of aqueous biphasic systems, J. Mol. Liq. 261 (2018) 250–264.